ECOSYSTEM ECOLOGY

Inferring biogenic and anthropogenic carbon dioxide sources across an urban to rural gradient

D. E. Pataki · T. Xu · Y. Q. Luo · J. R. Ehleringer

Abstract We continuously monitored CO_2 concentrations at three locations along an urban-to-rural gradient in the Salt Lake Valley, Utah from 2004 to 2006. The results showed a range of CO_2 concentrations from daily averages exceeding 500 p.p.m. at the city center to much lower concentrations in a non-urbanized, rural region of the valley. The highest values were measured in the wintertime and under stable atmospheric conditions. At all three sites, we utilized weekly measurements of the C and O isotope composition of CO_2 for a 1-year period to evaluate the CO_2 sources underlying spatial and temporal variability in CO_2 concentrations. The results of an inverse analysis of CO_2 sources and the O isotope composition of ecosystem respiration ($\delta^{18}O_R$) showed large contributions (>50%) of natural gas combustion to atmospheric CO_2 in the wintertime, particularly at the city center, and large contributions (>60%) of biogenic respiration to atmospheric CO_2 during the growing season, particularly at the rural site. $\delta^{18}O_R$ was most enriched at the rural site and more isotopically depleted at the urban sites due to the effects of irrigation on ecosystem water pools at the urban sites. The results also suggested differences in the role of leaf versus soil respiration between the two urban sites, with seasonal variation in the contribution of leaf respiration at a residential site and relatively constant contributions of leaf respiration at the city center. These results illustrate that spatial and temporal patterns of urban CO_2 concentrations and isotopic composition can be used to infer patterns of energy use by urban residents as well as plant and soil processes in urban areas.

Keywords Urban ecology · Carbon isotopes · Oxygen isotopes · Respiration · Fossil fuel emissions

D. E. Pataki (✉)
Department of Earth System Science and Department of Ecology and Evolutionary Biology,
University of California, Irvine, CA 92697, USA
e-mail: dpataki@uci.edu

T. Xu · Y. Q. Luo
Department of Botany and Microbiology,
University of Oklahoma, Norman, OK 73019, USA

J. R. Ehleringer
Department of Biology, University of Utah,
Salt Lake City, UT 84112, USA

Introduction

Human-dominated ecosystems play an increasing role in regional C cycles, leading to interest in the study of land–atmosphere exchange of CO_2 in cities. The urban to rural gradient of CO_2 concentrations in and surrounding cities has been referred to as the urban CO_2 "dome" (Idso et al. 1998, 2001). Energy use inventories, measurements of soil respiratory fluxes, and measurements of the isotopic composition of CO_2 have shown that elevated CO_2 in urban atmospheres originates from a number of sources, including gasoline combustion, natural gas combustion, and CO_2 of biogenic origin (Clark-Thorne and Yapp 2003; Day et al. 2002; Florkowski et al. 1998; Koerner and Klopatek 2002; Pataki et al. 2003a, 2005a). The spatial and temporal variability in these sources has not been well-studied, but this information is important for improving our understanding of spatial and temporal patterns

of energy and fuel use by urban residents, and also to quantify the role of plant and soil processes in urban areas, which is particularly poorly constrained (Pataki et al. 2006a).

In a previous study, we showed that a mass balance approach utilizing measurements of urban CO_2 concentrations, the C isotope ratio ($\delta^{13}C$) and O isotope ratio ($\delta^{18}O$) of CO_2, and the isotope ratio of local CO_2 sources can be applied toward partitioning CO_2 sources into their component parts (Pataki et al. 2003a). The basis of this method is the difference in $\delta^{13}C$ of natural gas versus gasoline combustion and in $\delta^{18}O$ of fuel combustion versus biogenic respiration. Limitations to this approach are sampling restrictions and two-end member assumptions associated with the Keeling plot method, which can distinguish between a background and a local CO_2 source if their proportions do not change during the measurement period (Keeling 1958, 1961; Pataki et al. 2003b). Using a tunable diode laser absorption spectrometer, we measured $\delta^{13}C$ of CO_2 at 5-min intervals and showed that the proportional contribution of fossil fuel sources does vary on a diurnal basis (Pataki et al. 2006b). In addition, the application

Table 1 List of abbreviations used in the text

C_B	Background CO_2 concentration
C_G	CO_2 concentration originating from gasoline combustion
C_N	CO_2 concentration originating from natural gas combustion
C_R	CO_2 concentration originating from respiration
C_T	Total ambient CO_2 concentration
K	Number of observations
P	Probability density function
e_a	Ambient vapor pressure
e_i	Intercellular vapor pressure
$\Delta^{18}O_E$	Enrichment of O isotopes at the site of enrichment relative to the plant water source
$\Delta^{18}O_V$	O isotopic composition of water vapor relative to the plant water source
$\delta^{13}C$	C isotope ratio
$\delta^{13}C_B$	C isotope ratio of background CO_2
$\delta^{13}C_G$	C isotope ratio of CO_2 derived from gasoline combustion
$\delta^{13}C_N$	C isotope ratio of CO_2 derived from natural gas combustion
$\delta^{13}C_R$	C isotope ratio of CO_2 derived from respiration
$\delta^{13}C_S$	C isotope ratio of local, non-background source CO_2
$\delta^{13}C_T$	C isotope ratio of atmospheric CO_2
$\delta^{18}O_B$	O isotope ratio of background CO_2
$\delta^{18}O_G$	O isotope ratio of CO_2 derived from gasoline combustion
$\delta^{18}O_N$	O isotope ratio of CO_2 derived from natural gas combustion
$\delta^{18}O_R$	O isotope ratio of CO_2 derived from respiration
$\delta^{18}O_S$	O isotope ratio of local, non-background source CO_2
$\delta^{18}O_T$	O isotope ratio of atmospheric CO_2
e^*	Equilibrium fractionation factor
e_k	Kinetic fractional factor
σ	SD

of O isotopes of CO_2 to partitioning biogenic and anthropogenic CO_2 sources requires a priori estimates of $\delta^{18}O$ of biological respiration ($\delta^{18}O_R$; see Table 1 for list of all abbreviations). In practice, $\delta^{18}O_R$ cannot be reliably measured in urban areas due to contamination from fossil fuel-derived CO_2, and can only be modeled with a number of assumptions regarding respiration rates and the isotopic composition of ecosystem water sources (Bowling et al. 2003; Lai et al. 2006b; Riley et al. 2003). Yet $\delta^{18}O_R$ contains information about ecological processes, particularly the relative contributions of above and belowground components of ecosystem respiration (Bowling et al. 2003). If the mass balance approach can be used without the limitations of the two-ended mixing model, and be can applied to solve for $\delta^{18}O_R$ rather than prescribe it, the magnitude and isotopic composition of the urban CO_2 "dome" can be used to make further inferences about urban ecosystem processes.

In this study we collected spatially and temporally intensive measurements of CO_2 concentrations, CO_2 isotopic composition, and water isotopic composition across an urban-to-rural gradient. Measurements were collected in the downtown business district, a residential neighborhood, and a non-urbanized, rural location in the Salt Lake Valley, Utah. The goals were to compare and contrast CO_2 concentrations, their isotopic composition, and their contributing sources across this urban-to-rural gradient. We also wished to further develop the isotopic mass balance approach to determine urban CO_2 sources for a wider range of conditions than permitted by the Keeling plot approach. This can allow the inference of $\delta^{18}O_R$ in order to estimate the contribution of above versus belowground respiration to total ecosystem respiration. Specifically, we hypothesized that:

1. Atmospheric CO_2 concentrations would decline from the city center to the residential neighborhood and the non-urbanized site.
2. Gasoline combustion would dominate CO_2 sources at the city center while natural gas combustion would dominate the residential site and biogenic respiration would dominate at the rural site.
3. Ecosystem water sources would be most enriched at the rural site in comparison to the two urban sites due to frequent irrigation with relatively isotopically depleted water at the urban sites.
4. Biogenic respiration at the city center would be dominated by leaf respiration due to the low proportion of pervious versus impervious surfaces.

To test these hypotheses in a coupled human–natural environment influenced both by plant and soil

Table 2 Location and elevation above sea level of the three measurement sites in the Salt Lake Valley, Utah

Site	Land cover	Coordinate location	Nearest cross streets	Elevation (m)
Eastern foothills	Residential	40°45′N, 111°50′W	1400 E, 200 S	1,430
Downtown	Commercial	40°45′N, 111°53′W	200 E, 300 S	1,320
Rural	Agricultural/shrubland	40°33′N, 112°03′W	Hwy 111, 9000 S	1,580

processes and by decision-making related to energy consumption and vegetation management, we collected an extensive dataset on the magnitude and variability in the urban CO_2 dome and its isotopic composition. We propose that these measurements have great potential for inferring patterns of human activities and biological respiration in complex, human-dominated ecosystems.

Materials and methods

CO_2 measurements

CO_2 concentrations and the isotopic composition of CO_2 were measured at three locations in the Salt Lake Valley: The University of Utah campus which is surrounded by a residential neighborhood, the Salt Lake City downtown business district, and a non-urbanized, rural region of the western valley characterized by mixed agricultural and natural sagebrush scrub land cover. These sites were referred to, respectively, as the Eastern foothills site, the Downtown site, and the Western foothills site in Pataki et al. (2005b), which showed a map of their locations. Coordinate locations, elevations, and street addresses of each site are shown in Table 2 and are described in detail in Pataki et al. (2005b). Measurements were conducted on the roof of four-story, ~18-m-high buildings at the Eastern foothills and Downtown sites. At the Western foothills site (which will be referred to here as a ''Rural'' site for clarity), roughness elements were much lower, such that measurements were taken from the top of a 9-m-tall meteorological tower.

CO_2 concentration measurements were conducted with infrared gas analyzers (LI-COR 7000 and LI-COR 6262; LI-COR, Lincoln, Neb.) and dataloggers (CR23x; Campbell Scientific, Logan, Utah), recording 2-min running averages every 5 min. Sampling was conducted according to Pataki et al. (2003a, 2005b) with the following exceptions: WMO-traceable calibration standards were introduced into the gas analyzers hourly at the Downtown and Rural sites rather than every 4 h to correct measurements to known values, as the instrumentation for these sites was located in outdoor, non-climate controlled enclosures. At the Eastern foothills site the instrumentation was located in a climate-controlled laboratory, and the calibration standard was introduced every 2 h. During 2005, we installed quality-control cylinders at each of the three sites to measure precision and accuracy of each system. The two outdoor systems (Downtown and Rural) had a precision of ±0.2 and ±0.4 p.p.m., respectively and an accuracy of +0.1 p.p.m.. The indoor system (Eastern foothills) had a precision and accuracy of ±0.2 and ±0.5 p.p.m. until September 2005 when an additional calibration standard was introduced to the system. This increased the precision and accuracy to ±0.1 and +0.03 p.p.m., respectively.

Sampling for $\delta^{13}C$ and $\delta^{18}O$ of CO_2 was similar to Pataki et al. (2003a, 2005b). Briefly, an automated sampler (Schauer et al. 2003) was used to fill sets of fifteen 100-ml glass flasks on a weekly basis from 0000 to 0500 hours mountain standard time (MST), using the same air inlets described for concentration measurements. This period was chosen because it commonly shows the greatest atmospheric stability, which is important in order to maximize sampling of local sources of CO_2. Air samples were dried with $Mg(ClO_4)_2$ prior to sampling and analyzed for $\delta^{13}C$ and $\delta^{18}O$ with continuous flow isotope ratio mass spectrometry (Delta Plus; Finnigan MAT, San Jose, Calif.) as described by Schauer et al. (2005). The precision of these measurements was 0.1‰ for $\delta^{13}C$ and $\delta^{18}O$ of CO_2 and 0.5 p.p.m. for concentration. Isotope ratios are expressed in δ notation referenced to Vienna Pee Dee belemnite for $\delta^{13}C$ and Vienna standard mean ocean water for $\delta^{18}O$.

Keeling plots of $\delta^{13}C$ and $\delta^{18}O$ of CO_2

For each sample period, Keeling plots were constructed to determine the C isotopic composition ($\delta^{13}C_S$) and O isotopic composition ($\delta^{18}O_S$) of local, non-background CO_2 (Keeling 1958, 1961; Pataki et al. 2003b). This method essentially removes the influence of background CO_2 with a two-ended, linear mixing model between background and local source CO_2. If

there are more than two sources of CO_2, as is generally the case in this study, this approach is only valid if the proportional contribution of each source does not change during the sampling period. Estimates of $\delta^{13}C_S$ and $\delta^{18}O_S$ were obtained by geometric mean regression with error bars derived from standard linear regression (Pataki et al. 2003b). Outliers were removed for datapoints with residuals more than 2 SDs from the mean (Bowling et al. 2002). Estimates were obtained only for statistically significant regressions at α = 0.05, $R^2 > 0.6$, and SEs <3‰. Using this filter, 87% of the sample sets at the two urban sites were retained for C isotopes, and 41% were retained for O isotopes. At the rural site, 47% of the sample sets were retained for C isotopes and only 10% were retained for O isotopes.

Inverse modeling

We applied a simple set of mass balance equations for determination of the magnitude of local CO_2 sources:

$$C_T = C_B + C_N + C_G + C_R \tag{1}$$

$$\delta^{13}C_T C_T = \delta^{13}C_B C_B + \delta^{13}C_N C_N + \delta^{13}C_G C_G + \delta^{13}C_R C_R \tag{2}$$

$$\delta^{18}O_T C_T = \delta^{18}O_B C_B + \delta^{18}O_N C_N + \delta^{18}O_G C_G + \delta^{18}O_R C_R \tag{3}$$

where C is CO_2 concentration, $\delta^{13}C$ C isotope ratio of CO_2, $\delta^{18}O$ O isotope ratio of CO_2, and the subscripts T, B, N, G, and R refer to total ambient CO_2, background CO_2, natural gas combustion, gasoline combustion, and biogenic respiration, respectively. In this application, background CO_2 refers to the CO_2 concentration of the atmosphere in the absence of local sources.

In this analysis, we solved for C_N, C_G, C_R, and $\delta^{18}O_R$, the most unconstrained of all the variables in Eqs. 1–3. The isotopic composition of local fuel sources can be directly measured, and we have characterized these values in previous studies (Bush et al. 2007; Pataki et al. 2003a, 2005a). The concentration and isotopic composition of the background atmosphere can be estimated with measurements from a National Oceanic and Atmospheric Administration Climate Monitoring and Diagnostics Laboratory (NOAA CMDL) monitoring station in Wendover, Utah, which corresponds well to the minimum, afternoon CO_2 concentration recorded at our urban sites during periods of large-scale atmospheric mixing (Pataki et al. 2006b). $\delta^{13}C_R$ has been measured

extensively in a variety of natural ecosystems, and is relatively well constrained in C_3-dominated ecosystems in comparison to the other sources of variability considered here. However, $\delta^{18}O_R$ varies greatly with the isotopic composition of the water sources of a particular ecosystem, because respiratory CO_2 in both plants and soils equilibrates with water (Gillon and Yakir 2001). Aboveground respiration is generally enriched relative to belowground respiration because CO_2 in leaves equilibrates with leaf water that has been enriched by transpiration of isotopically light water (Farquhar and Lloyd 1993; Farquhar et al. 1993). Belowground respiration is generally more depleted because soil CO_2 equilibrates with shallow soil water at about 5–15 cm depth that is not as evaporatively enriched as leaf water (Flanagan et al. 1996; Miller et al. 1999). If the isotopic variation of local water sources is known, $\delta^{18}O_R$ can be modeled as a function of the climatic variables that drive evaporative enrichment, but only if the proportional contributions of leaf and soil respiration are known. In the past, we assumed a constant, arbitrary value for the partitioning between leaf and soil respiration, so that we could use Eqs. 1–3 to solve for C_G, C_N, and C_R (Pataki et al. 2003a).

As an alternative, in the current study we used an inverse modeling approach to solve for four unknowns: C_N, C_G, C_R, and $\delta^{18}O_R$. For the end members, we specified $\delta^{13}C_G = -28‰$ and $\delta^{13}C_N = -37‰$ from previous studies in the Salt Lake Valley that characterized the isotopic composition of fossil fuel sources from direct measurements (Bush et al. 2007; Pataki et al. 2005a, 2006b). $\delta^{18}O_G$ and $\delta^{18}O_N$ were assumed to be equivalent to the theoretical value of 23.5‰ (the isotopic composition of atmospheric O_2) due to the difficulty of measuring these values directly without experimental artifacts caused by condensation. While there is a possibility that actual and theoretical values differ, these effects are likely to be small relative to the range of possible values and uncertainties in $\delta^{18}O_R$ (Pataki et al. 2003a, 2005a). For $\delta^{13}C_R$, a mean value for C_3 ecosystems of $-26‰$ was specified. C_B was estimated from measurements at the NOAA CMDL monitoring station in Wendover, about 200 km to the west of the Salt Lake Valley (Globalview-CO_2 2005). $\delta^{13}C_B$ and $\delta^{18}O_B$ were specified as average observed values of -8.5 and 41‰, respectively (Pataki et al. 2005b).

For Bayesian prior constraints on the unknown variables, C_R, C_G, and C_N were each restricted to $0 \leq C_N, C_G, C_R \leq$ maximum($C_T - C_B$) with ($C_R + C_G + C_N$) = ($C_T - C_B$). For $\delta^{18}O_R$, the isotopic composition of total ecosystem respiration is expected to fall between

the values for isotopically enriched aboveground respiration and relatively depleted belowground respiration (Flanagan et al. 1996). For CO_2 equilibrated with leaf water, we modeled the isotopic composition of leaf water using the modified Craig–Gordon equation:

$$\Delta^{18}O_E = e^* + e_k + (\Delta^{18}O_V - e_k)(e_a/e_i) \tag{4}$$

where $\Delta^{18}O_E$ is enrichment of water at the site of evaporation, e^* temperature-dependent equilibrium fractionation in evaporation, e_k kinetic fractionation of diffusion, $\Delta^{18}O_V$ isotope ratio of water vapor in air relative to the plant's water source, and e_a/e_i ratio of vapor pressure outside and inside the leaf (Craig and Gordon 1965; Flanagan et al. 1991, 1997). This is a steady state model that does not consider potential changes in leaf water content, as will be discussed further. For these calculations, we used the mean observed value for atmospheric water vapor in 2004 of −23‰ measured as described below and temperature and relative humidity data reported by the NOAA MesoWest monitoring station (http://www.met.utah.edu/mesowest/) location nearest to each of our study sites.

Prior estimates of the maximum (max.; most enriched) expected $\delta^{18}O$ of leaf respiration and minimum (min.; most depleted) expected values of $\delta^{18}O$ of soil respiration were applied, such that: min.(soil $\delta^{18}O$) ≤ $\delta^{18}O_R$ ≤ max.(leaf $\delta^{18}O$). These values were modeled with estimates of the isotopic composition of source water. In the Salt Lake Valley, winter snowmelt is the dominant source of groundwater, surface water, and urban irrigation water, with an average $\delta^{18}O$ of approximately −15‰. Therefore, the most depleted expected value for soil water is −15‰. To allow for some possible enrichment of plant source water, we used a source value of −10‰ in Eq. 4. The prior constraints for the isotopic composition of $\delta^{18}O_R$ were then specified by modeling leaf water enrichment with Eq. 4 and assuming temperature-dependent equilibration between CO_2 and with soil water or modeled leaf water according to Majoube (1971).

Using these prior values, a Bayesian probabilistic inversion technique (Leonard and Hsu 1999; Tarantola 2005) was used to solve for C_N, C_G, C_R, and $\delta^{18}O_R$ in Eqs. 1–3. For this purpose, a prior probability density function (PDF) effectively defines the range of the estimates. A uniform distribution assumes that any value in the defined range is equally likely. For each of the observation periods, C_N, C_G, C_R, and $\delta^{18}O_R$ were specified as:

$$J(C_N,C_G,C_R,\delta_R^{18}) = \sum_{i=1}^{K}\left(C_N + C_G + C_R - (C_{T,i} - C_{B,i})\right)^2 /\sigma_1^2$$

$$+\sum_{i=1}^{K}\left(\delta_N^{13}C_N + \delta_G^{13}C_G + \delta_R^{13}C_R - (\delta_{T,i}^{13}C_{T,i} - \delta_R^{13}C_{B,i})\right)^2 /\sigma_2^2$$

$$+\sum_{i=1}^{K}\left(\delta_N^{18}C_N + \delta_G^{18}C_G + \delta_R^{18}C_R - (\delta_{T,i}^{18}C_{T,i} - \delta_B^{18}C_{B,i})\right)^2 /\sigma_3^2$$

$$P \propto \exp\left\{-\frac{1}{2}J(C_N,C_G,C_R,\delta_R^{18})\right\} \tag{5}$$

where P represents the PDF for C_N, C_G, C_R, and $\delta^{18}O_R$, α proportionality, and K number of observations in each period. Constants σ_1, σ_2, and σ_3, SD of, $C_T–C_B$, $\delta_T^{13}C_T–\delta_R^{13}C_B$ and $\delta_T^{18}C_T–\delta_B^{18}C_B$ and are used to normalize the difference between simulated data and observed data in function J.

A Metropolis–Hastings algorithm (Gelfand and Smith 1990; Gelman and Rubin 1992; Geman and Geman 1984; Gill 2002; Hastings 1970) was used to obtain samples from Eq. 5 in order to make a mean estimation for the unknown parameters C_N, C_G, C_R, and $\delta^{18}O_R$ for each time period. The algorithm was run by repeating two steps: a proposing step and a moving step. In each proposing step, the algorithm generated a new estimation based on a previous estimation according to a uniform proposal probability distribution. The new estimation was tested against the Metropolis criterion to determine if it should be accepted or rejected. The mean estimation was based on about 5,000 accepted samples of the PDF. A similar application of this method with detailed procedures of the Metropolis–Hastings algorithm was described by Xu et al. (2006).

Ecosystem water measurements

The isotopic composition of water vapor was measured weekly at the Eastern foothills site from the same air inlets as the CO_2 measurements. Samples were collected by condensing water vapor in a cold trap placed in a dry ice–ethanol slush. A long sampling period was chosen from 1200 to 1700 hours MST in order to ensure sufficient sample sizes during the dry summer period. Water samples were analyzed for $\delta^{18}O$ by online pyrolysis (TC EA and Delta Plus; Finnigan MAT) according to Gehre et al. (2004).

During the growing season, leaf, stem and soil samples were also collected for water extraction and

Fig. 1 Mean daily CO_2 concentrations at three sites in the Salt Lake Valley, Utah. *Eastern Foothills* University of Utah campus, *Downtown* Salt Lake City downtown business district, *Rural* non-urbanized, rural region
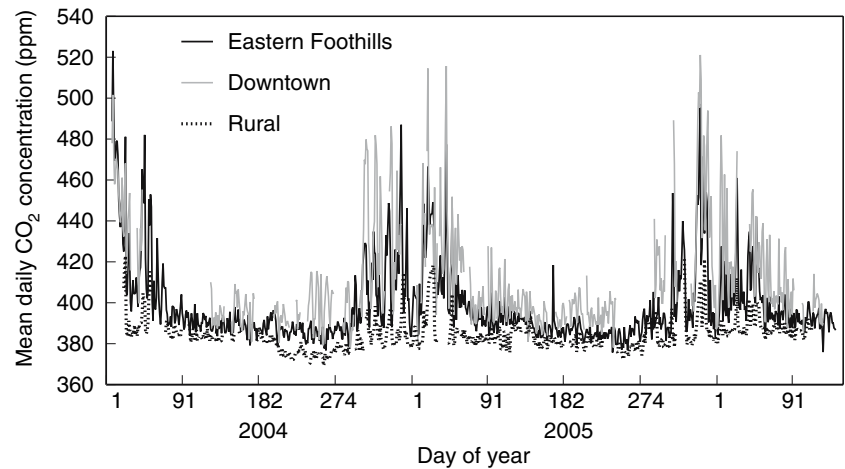
Fig. 2 The hourly ensemble average CO_2 concentration at the three sites in January and July of 2005. For sites, see Fig. 1
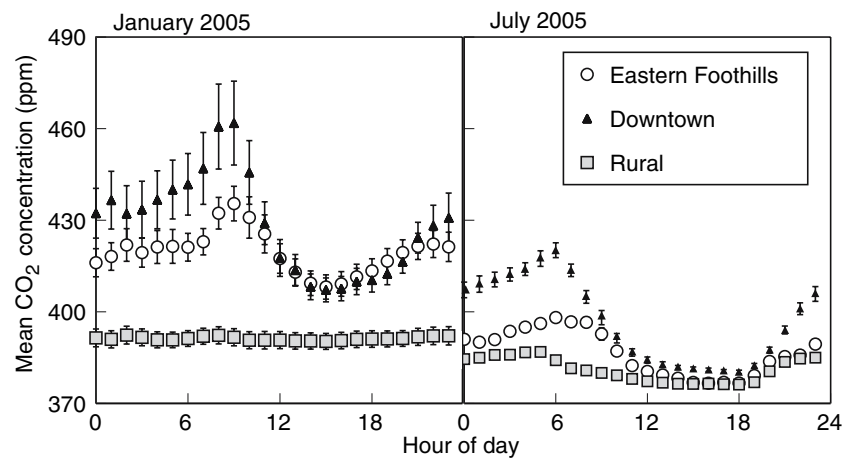

isotopic analysis from the three study sites every 2 weeks during midday. At the Eastern foothills sites, leaf and stem samples were collected from six individuals of *Pinus* spp. and six deciduous species: three *Gleditsia triacanthos* and three *Tilia cordata*. Six soil samples were collected at 10-cm depth. At the Western foothills site, leaf and stem samples were collected from six individuals of *Artemisia tridentata* and six soil samples were collected from 10-cm depth. At the Downtown site, six leaf and stem samples were collected from *G. triacanthos* as well as an additional six samples from *Acer platanoides*. Soil samples were not collected downtown as trees were grown in small planters or sidewalk cutouts and very little exposed soil was available. All samples were collected in vacutainers, parafilmed, and frozen until extraction by cryogenic vacuum distillation (West et al. 2006) and analyzed by online pyrolysis (TC EA and Delta Plus; Finnigan MAT).

Results

Atmospheric CO_2 concentrations

Mean daily CO_2 concentrations from January 2004 to May 2006 showed the expected seasonal cycle with the highest concentrations during wintertime inversions (Fig. 1). Among sites, the Rural site consistently showed the lowest concentrations while the Downtown site showed the highest. At the two urban sites, 24-h average CO_2 concentrations occasionally exceeded 500 p.p.m. in the wintertime (Fig. 1). Differences among sites were even more apparent in the average diurnal patterns in January versus July. In January 2005, the Downtown site showed the highest CO_2 concentrations at night, but was similar to the Eastern foothills site in the daytime, while the Rural site showed consistently lower and relatively constant values (Fig. 2). This pattern was maintained in July 2005,

Fig. 3 The isotopic composition of local, non-background CO_2 ($\delta^{13}C_S$ and $\delta^{18}O_S$) as estimated by the Keeling plot method (Keeling 1958, 1961; Pataki et al. 2003b). For sites, see Fig. 1. *VSMOW* Vienna standard mean ocean water, *VPDB* Vienna Pee Dee belemnite
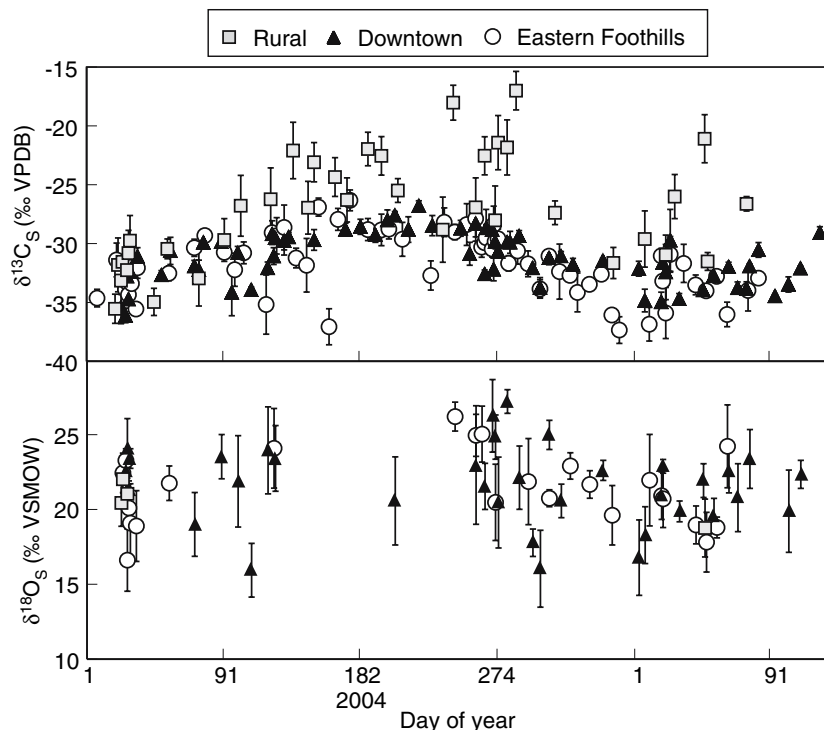
although absolute CO_2 concentrations were lower at all three sites, particularly during afternoon, well-mixed atmospheric conditions (Fig. 2).

The isotopic composition of CO_2

The isotopic composition of local, nighttime CO_2 sources as estimated with the Keeling plot method also showed a seasonal cycle (Fig. 3). For C isotopes, the Keeling plot intercept ($\delta^{13}C_S$) was most depleted in the wintertime and heaviest during summer (Fig. 3, upper panel). Among sites, the Rural site showed the heaviest values, with $\delta^{13}C_S$ exceeding the range of possible combustion and C_3 plant respiratory sources during the growing season (Fig. 3, upper panel). For O isotopes, there was some indication of a seasonal cycle at the two urban sites (Fig. 3, lower panel), but during the growing season there was too much scatter in the relationship between CO_2 concentrations and isotopic composition to derive $\delta^{18}O_S$, such that Keeling plots during this period were not statistically significant. For the Rural site, which generally showed lower CO_2 concentrations than the urban sites (Figs. 1, 2), Keeling plots were rarely statistically significant for O isotopes ($P > 0.05$).

As an alternative to using Keeling plots to account for the influence of the background on local CO_2, we applied an inverse analysis to Eqs. 1–3 to solve for C_R, C_G, C_N and $\delta^{18}O_R$. The results showed reasonable and

intuitive patterns, with 20–60% of nighttime, local CO_2 originating from biogenic respiration during the growing season, in contrast to 0–40% contributions of biogenic respiration during winter, depending on location (Fig. 4a). Biogenic respiration made the largest contribution to local CO_2 at the Rural site and the smallest contribution at the Downtown site (Fig. 4a). In contrast, natural gas combustion made the largest contribution to nighttime CO_2 at the Downtown site in winter and the smallest contribution at the rural site in summer (Fig. 4c). The proportional contribution of gasoline combustion remained relatively constant throughout the year (Fig. 4b). For clarity, error estimates are not shown in Fig. 4, but are shown in Fig. 5 as a function of the magnitude of the estimated percent contribution of C_R, C_N, and C_G to total CO_2. The SDs of the estimates were not randomly distributed, but increased as the magnitude of the estimates decreased (Fig. 5). In other words, there was a large uncertainty (>50% relative error) associated with the inverse model results when a given CO_2 source was a small (<30%) contributor to local CO_2. Therefore, the most robust estimates of C_R in Fig. 4 occur during the growing season and the most robust estimates of C_N occur in the winter.

For model validation, measured and modeled $\delta^{13}C_T$ were compared and found to be in very good agreement (Fig. 6). Therefore, we further utilized the model
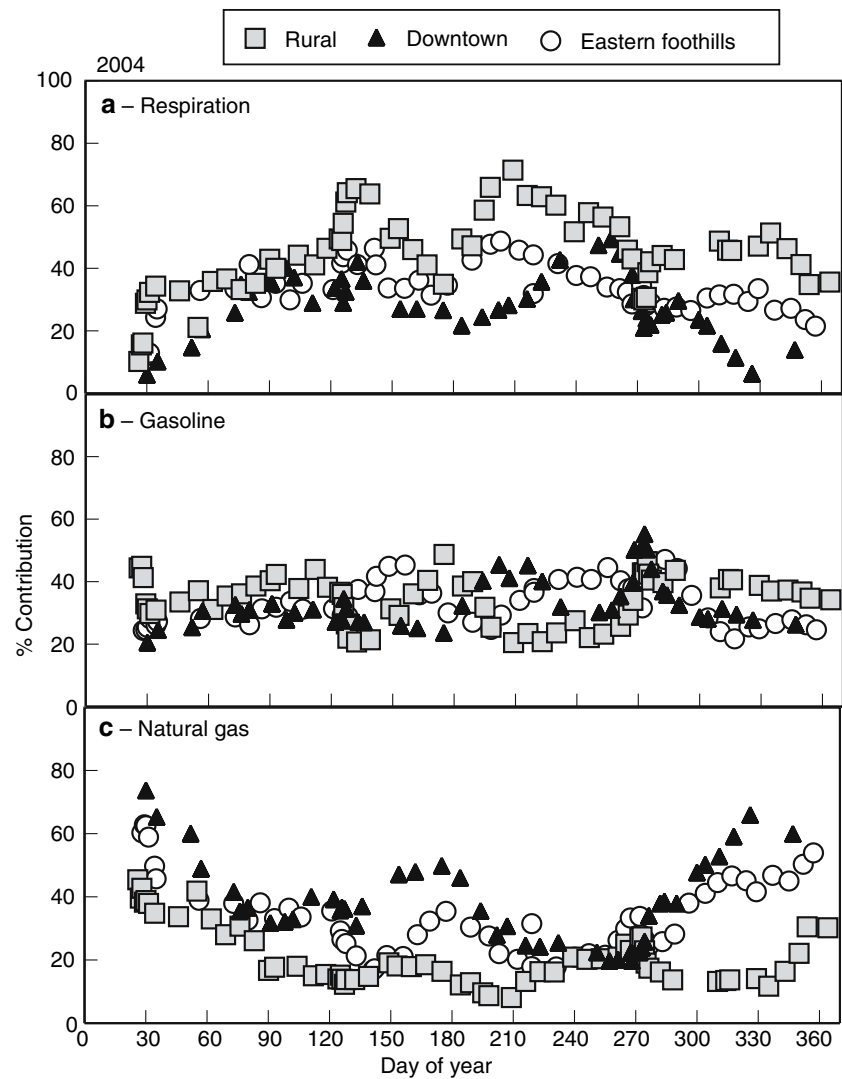
to evaluate the model estimates of $\delta^{18}O_R$, which
showed some seasonality, particularly at the Rural site
(Fig. 7). There was a trend toward higher, more en-
riched values of $\delta^{18}O_R$ overall at the Rural site, and for
more depleted values following summer precipitation,
although these differences were not distinguishable
based on the SD of the estimates (Fig. 7). The seasonal
pattern in $\delta^{18}O_R$ was not explained by effects of sea-
sonality in the isotopic composition of water vapor on
leaf water enrichment, as $\delta^{18}O$ of water vapor showed
weekly variability but not on a seasonal basis (Fig. 7).

The isotopic composition of local water sources

There was some seasonality in ecosystem water sources
during the growing season that would subsequently
affect $\delta^{18}O_R$. At the urbanized Eastern foothills site,
$\delta^{18}O$ of soil water at 5-cm depth became more

enriched, from –13.1 ± 0.3‰ in May to –10.2 ± 0.9‰ in
October. Stem waters followed this trend, but were
more depleted overall (Fig. 8) due to plant water up-
take from lower depths. Stem waters at the Downtown
site were similar to those at the Eastern foothills site
(Fig. 8). The Rural site showed a different pattern of
stem, soil and leaf water than the urbanized sites
(Fig. 8), presumably because this site is not irrigated
and relies on lower elevation precipitation and spring
snowmelt as the plant and soil water source. Average
soil water $\delta^{18}O$ at this site ranged from –9.3 ± 0.6‰ in
June to –0.7 ± 2.1‰ in August, with stem waters more
depleted but largely mirroring soil water variability
(Fig. 8).

Midday leaf waters were much more enriched than
stem waters (Fig. 8) as expected during periods of
transpiration. We compared measured $\delta^{18}O$ of bulk
leaf water to $\delta^{18}O$ of water at the site of evaporative
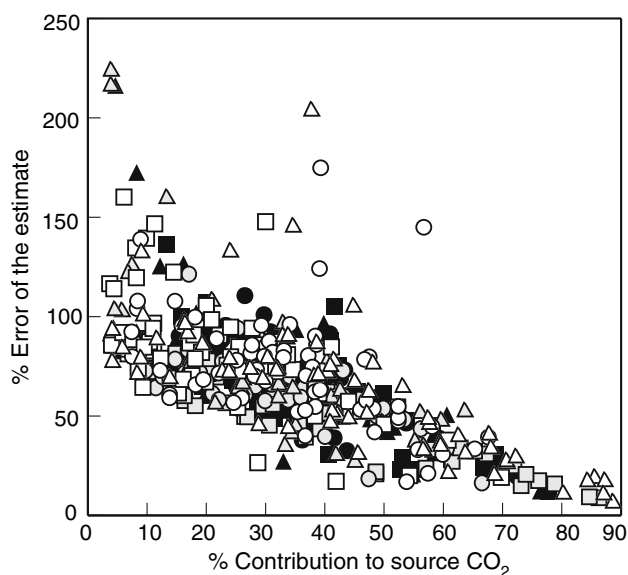
Fig. 5 The percent error of the inverse modeling estimates as a function of the estimates shown in Fig. 3. The *open symbols* show the Rural site, *grey symbols* show the Downtown site, and *closed symbols* show the Eastern foothills site. The percent contribution of natural gas combustion is shown in *squares*, gasoline combustion in *circles*, and respiration in *triangles*. For sites, see Fig. 1

enrichment as modeled with Eq. 4. Overall, there was good agreement for the Eastern foothills and Rural sites (Fig. 9). For the Downtown site there were species-specific effects, with *G. triacanthos* more depleted than predicted and *A. platanoides* heavier than predicted for most sample collection periods (Fig. 9).

Contributions of aboveground versus belowground respiration

As there was reasonable agreement between modeled and measured leaf water, we used the estimates of $\delta^{18}O_R$ derived from the inverse analysis to evaluate the potential proportional contributions of leaf versus soil respiration to total biogenic respiration. We estimated

$\delta^{18}O$ of soil respiration from the mean observed value of $\delta^{18}O$ of soil water observed at each site and the temperature-dependent equilibration between CO_2 and water (Majoube 1971). Similarly, we modeled $\delta^{18}O$ of leaf respiration from the mean of observed value of $\delta^{18}O$ of stem water and Eq. 4. We then estimated the proportional contribution of leaf respiration to $\delta^{18}O_R$ assuming that leaf and soil respiration were the only possible sources, (i.e., stem respiration was neglected). For error estimates, the SD of estimated $\delta^{18}O_R$ was propagated with the SD of measured leaf and soil water. Because there was a great deal of variability in $\delta^{18}O$ of water sources at the Rural site, this resulted in very large estimated errors, sometimes exceeding 100% relative error. Therefore, the results are shown only for the two urban sites in Figs. 10, 11.

There was a seasonal pattern in the proportional contribution of leaf respiration at the Eastern foothills site, with relatively small contributions of <30% in winter and large contributions of 40–80% in mid summer (Fig. 10). At the Downtown site, there was a relatively constant contribution of approximately 50% leaf respiration during all periods, with the exception of March–April, when leaf respiration constituted only about 20% of total ecosystem respiration.

Discussion

Atmospheric CO_2 across the urban to rural gradient

The seasonal cycle of atmospheric CO_2 concentrations at the Eastern foothills site observed in 2002 (Pataki et al. 2003a) persisted in subsequent years (Fig. 1). Elevated wintertime CO_2 concentrations can often be attributed to the effects of atmospheric temperature inversions that result in the accumulation of urban CO_2 throughout the Salt Lake Valley (Pataki et al. 2005b). Near-ambient CO_2 concentrations in the summertime are likely due to increased convection and photosyn-

Fig. 6 Comparison of measured values of isotopic composition of atmospheric CO_2 ($\delta^{13}C_T$) with inverse modeling estimates at each site. The *dotted line* is the 1:1 line. For sites, see Fig. 1
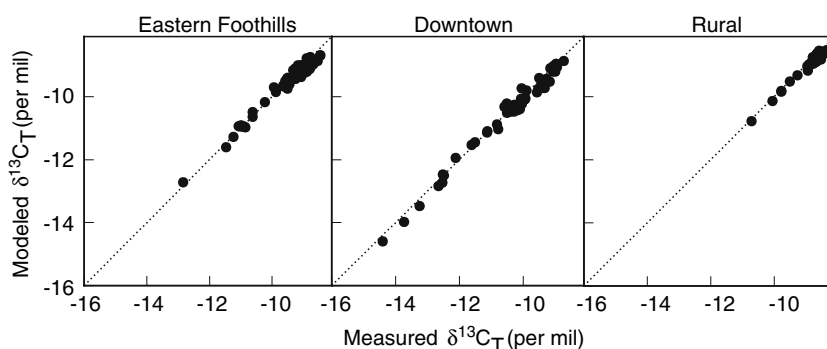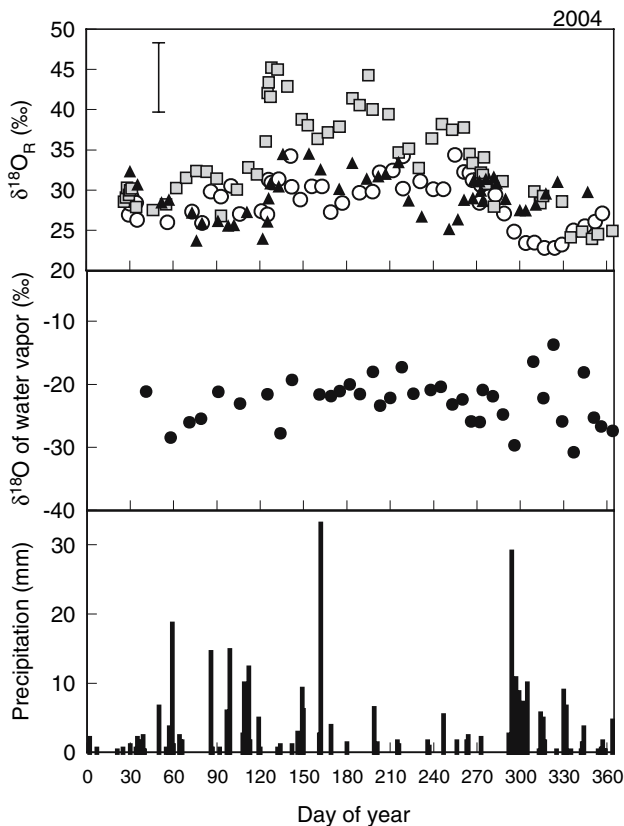
Fig. 7 *Top panel* Five interval running average of the O isotope composition of ecosystem respiration ($\delta^{18}C_R$) for each site as estimated by inverse modeling. The *error bar* shows the average SD for all estimates. *Middle panel* The O isotope composition ($\delta^{18}O$) of atmospheric water vapor at the Eastern foothills site collected from 1200 to 1700 hours mountain standard time. *Bottom panel* Precipitation for the same period measured by the National Oceanic and Atmospheric Administration MesoWest network (http://www.met.utah.edu/mesowest/), station WBB, which is adjacent to the Eastern foothills site

thetic CO_2 drawdown. In the summertime, CO_2 concentrations were often similar at all three sites during the daytime (Fig. 2). With regard to spatial variability, the CO_2 concentration record showed the hypothesized urban CO_2 "dome" effect, with the highest concentrations of CO_2 consistently observed downtown and the lowest at the non-urbanized Rural site (Figs. 1, 2). This spatial pattern was most pronounced during nighttime, stable atmospheric conditions (Fig. 2).

Variability in CO_2 sources

We utilized the isotopic composition of elevated local CO_2 concentrations to infer aspects of the urban ecosystem C cycle. Keeling plot intercepts for C isotopes of CO_2 showed a seasonal pattern that was very similar at the two urban sites, but more isotopically enriched

at the non-urbanized Rural site (Fig. 3). This was likely indicative of: (1) a smaller contribution of natural gas combustion to atmospheric CO_2 at the Rural site, and (2) a contribution of C_4 plant-derived organic matter to respiratory CO_2 fluxes. Gasoline combustion is likely to make a larger contribution to CO_2 at the Rural site than natural gas combustion, as there are several roads in the vicinity of the sampling site but no residences, buildings, or other possible sources of natural gas combustion. Respiration of C_4 plant material may derive from the very small proportion of C_4 plant species found in the surrounding sagebrush scrub land cover, or from previous cropping with corn in the agricultural portions of the site. However, historical records for the site indicate previous cropping with C_3 wheat and alfalfa. We are not aware of industrial or other enriched possible sources of CO_2 in the immediate vicinity, although periodic advection from more remote sources may be possible. We suggest that the more likely explanation for the enriched $\delta^{13}C_S$ values outside of the range of possible CO_2 sources at the Rural site is violations in the assumptions of the Keeling plot method and resulting errors in the estimate.

In this study, the Keeling plot approach was limited in its usefulness for estimating $\delta^{13}C_S$ and $\delta^{18}O_S$ and for distinguishing between biogenic and anthropogenic CO_2 sources for several reasons. Firstly, it was difficult to obtain statistically significant relationships between CO_2 concentrations and isotope composition, particularly for O. This difficulty has been noted previously for natural ecosystems (Bowling et al. 2003; Harwood et al. 1999; Lai et al. 2006b; Mortazavi and Chanton 2002; Sternberg et al. 1998), and is compounded here due to the presence of additional combustion-derived CO_2 sources as well as above and belowground respiration, which have very different O isotope compositions. In addition, we have shown previously that CO_2 sources vary diurnally at the residential site in wintertime (Pataki et al. 2006b) and this is likely true for the other sites during other periods of the year. In that study, the contribution of natural gas combustion to CO_2 sources peaked in early morning hours due to residential heating versus traffic contributions. Integrated during our sampling period of 0000–0500 hours, the average fraction of natural gas combustion was relatively similar to the 24-h average in our previous study (Pataki et al. 2006b); however, when the proportional contribution of CO_2 sources changes during the Keeling plot sampling period, the estimates are associated with a high degree of error and may result in intercepts outside of the range of any local sources (Pataki et al. 2003a).

Fig. 8 $\delta^{18}O$ of soil water at 10-cm depth and leaf and stem water for *Tilia cordata*, *Gleditsia triacanthos*, *Pinus* spp., *Acer platanoides*, and *Artemisia tridentata*. *Error bars show the SE; some are smaller than the symbols. For sites see Fig.* 1; *for abbreviations, see Fig.* 7
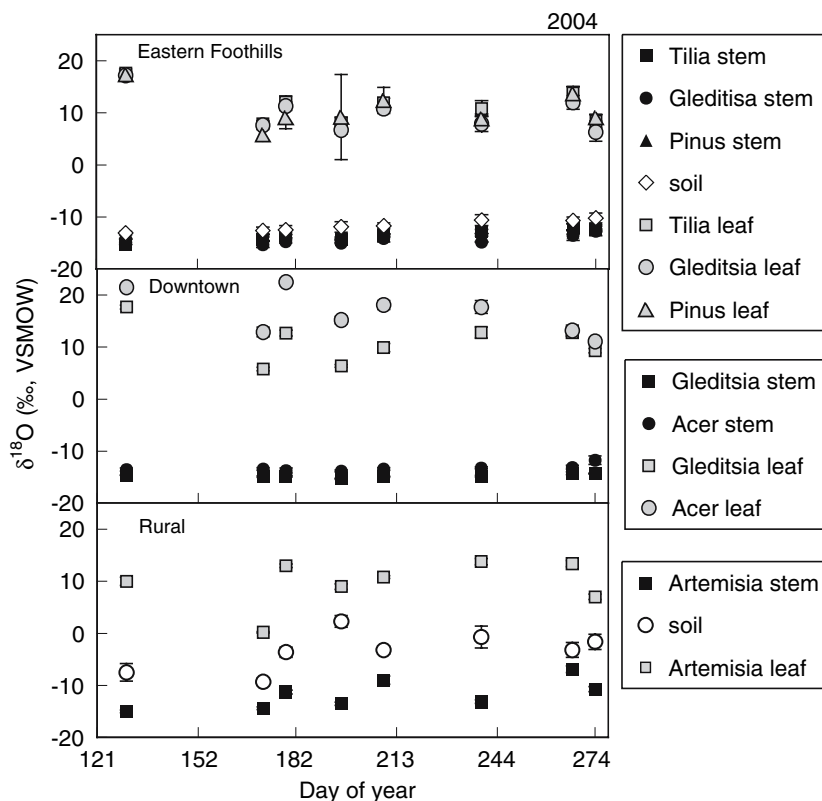

The inverse modeling approach provided a useful alternative, albeit one with some caveats. The results shown in Fig. 4 followed hypothesized trends in that biogenic respiration was highest at the Rural site and lowest at the Downtown site. However, natural gas combustion was highest at the Downtown site rather than at the Residential site, contrary to the original hypothesis. This implies that natural gas combustion for heating played a larger role than expected at the Downtown site relative to gasoline combustion. It should be noted that if C_4-derived plant or soil respiration is in fact important at the Rural site, the prescribed value of $\delta^{13}C_R$ of $-26‰$ is probably too depleted. This would result in an over-estimation of the proportional contribution of gasoline combustion and an under-estimation of the proportional contribution of natural gas combustion to the total. There is also likely to be temporal variability in $\delta^{13}C_R$ in response to climatic variability that was unaccounted for, although these variations may be relatively small in comparison to the error of the estimates. The error analysis in Fig. 5 showed that the inverse method only yielded relatively low errors of <30% relative error when a given CO_2 source dominated the total local source. Estimated contributions from less important CO_2 sources, (e.g., biogenic respiration during wintertime or natural gas

combustion during summer) were associated with a very high degree of error. Hence, this method appears to be most useful for assessing patterns of dominant urban CO_2 sources.

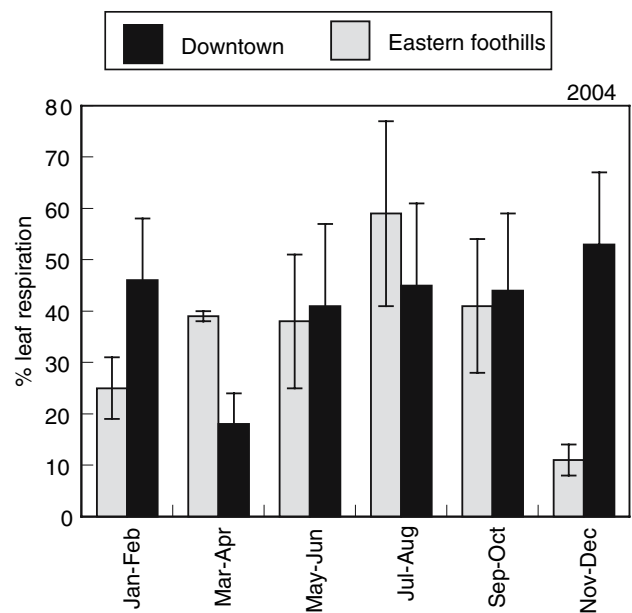Isotopic enrichment of water pools across the urban to rural gradient

At the non-urbanized site, plant and soil water isotopic composition followed common trends for natural ecosystems: $\delta^{18}O$ of shallow soil water became progressively enriched until mid July; however, stem water isotopes were considerably more depleted (Fig. 8) because plant water sources originated from deeper, non-enriched water. Exceptions were 27 July and 23 September, when stem water isotopes appeared to reflect uptake of enriched local, monsoonal precipitation. In contrast, both soil and stem water isotopes at the urbanized sites remained relatively depleted throughout the growing season (Fig. 8) due to continued irrigation as hypothesized. The two urban sites showed about 2‰ enrichment of plant and soil water pools during the growing season, while the non-urbanized site showed temporal variability in the isotopic composition of water late in the season without a clear seasonal trend (Fig. 8). This is likely because irrigation at the
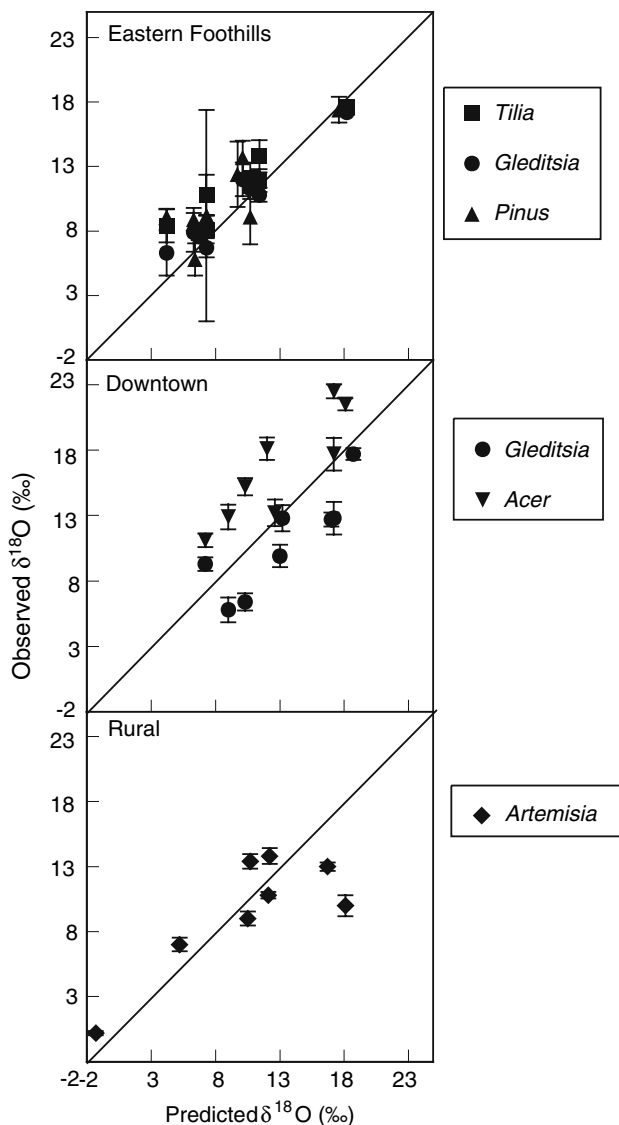
Fig. 9 The observed $\delta^{18}O$ of leaf area versus values predicted by Eq. 4. The *line* is the 1:1 line. *Error bars* show the SE. Species names are given in Fig. 8; for sites, see Fig. 1

Fig. 10 The percent contribution of leaf respiration to total ecosystem respiration. *Error bars* show the SD propagated as described in the text. For sites, see Fig. 1

two urban sites became insufficient to maintain constant shallow soil moisture and isotopic composition as the dry summer season progressed. At the non-urbanized site, winter snowmelt was likely to be largely absent from the shallow soil by July, after which plant and soil water pools were more influenced by summer monsoonal precipitation events (Fig. 5) than at the two urbanized sites.

At the downtown site, there were species differences in leaf water enrichment that were not reflected in stem water isotopic composition (Fig. 8). Leaf water $\delta^{18}O$ of *G. triacanthos* was generally more depleted than predicted by the Craig–Gordon model, while *A. platanoides* was more enriched (Fig. 9). Bulk leaf water

enrichment which was less than predicted may be attributable to the Péclet effect, or mixing of enriched and unenriched water, as well as to non-steady effects involving changes in leaf water content (Cernusak et al. 2002; Farquhar and Gan 2003; Farquhar and Lloyd 1993; Lai et al. 2006a). For *Acer*, which has much larger leaves than *Gleditisia*, under-prediction of leaf water enrichment may have been caused by under-estimation of e_i, which was calculated with the assumption that leaf and air temperature were equivalent. In fact, leaf temperature in *Acer* may have been higher than air temperature during midday sampling.

Estimating sources of ecosystem respiration with O isotopes

The Bayesian approach for solving for $\delta^{18}O_R$ appears to be very promising for improving our understanding of overall patterns of urban ecosystem function, particularly with respect to better understanding urban plant and soil respiration. We have previously been unable to measure $\delta^{18}O_R$ directly, due both to difficulty in applying the Keeling plot approach for O and also because of contamination from fossil fuel-derived CO_2 in urban areas. With the inverse modeling approach, we placed relatively large prior constraints on $\delta^{18}O_R$ and inferred the optimal set of solutions to the mass balance. The resulting seasonal pattern of $\delta^{18}O_R$ shown in Fig. 7 has two components: increased enrichment of

Fig. 11 The frequency distribution of estimates of CO_2 concentration originating from natural gas combustion (C_N), CO_2 concentration originating from gasoline combustion (C_G), CO_2 concentration originating from respiration (C_R), and $\delta^{18}O_R$ for 21 January 2004 at the Residential site as described in Appendix 1
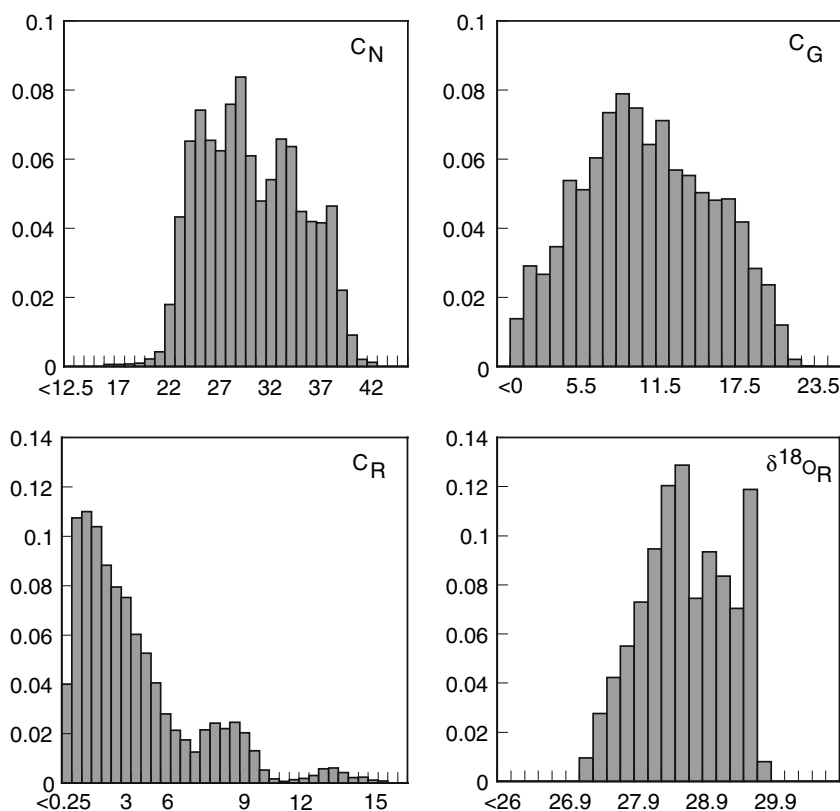
ecosystem water pools during summer months as discussed above as well as shifts in the contribution of aboveground versus belowground respiration to total ecosystem respiration.

The partitioning between above- and belowground respiration shown in Fig. 10 is associated with several potential sources of uncertainty. Sources of error not captured in the error bars of the estimates include: (1) non-steady state leaf water enrichment caused by changing leaf water content, and (2) the difference between the effects of net CO_2 efflux from leaves (considered in this analysis) and one-way fluxes (the true influence on $\delta^{18}O$ of leaf respiratory CO_2). With regard to (1), measured and Craig–Gordon modeled leaf water showed reasonable agreement during the daytime (Fig. 9) but at night, bulk leaf water can depart considerably from that predicted by Eq. 4 (Cernusak et al. 2002, 2005; Farquhar and Cernusak 2005). This may cause an error of several per mil in the estimation of leaf water enrichment. However, the effect of (2) may cause an error of several hundred per mil in the estimation of the isotopic composition of leaf-respired CO_2 (Cernusak et al. 2004). This is because CO_2 may diffuse into leaves, equilibrate with leaf water, and diffuse back to the atmosphere at night if stomata are not fully closed. Barbour et al. (2005)

found that for *Quercus rubra*, a common street tree species in the Salt Lake Valley, this effect was large near sunrise and sunset, and less significant during other periods. Non-steady state and gross flux refinements to models of leaf water enrichment and respiratory CO_2 are relatively recent and their importance in a range of natural and managed ecosystems is not yet known. A limitation to current models of both non-steady state leaf water enrichment and the one-way flux of leaf respiratory $\delta^{18}O$ is that estimates of nighttime stomatal conductance are required. For long-term, continuous monitoring of relatively large areas as in the current study, obtaining continuous, whole canopy estimates of nighttime conductance is very difficult. For example, sap flux measurements of whole plant transpiration cannot be applied toward estimating conductance during conditions of low evaporative demand (Ewers and Oren 2000), as is commonly the case at night.

For the purposes of this study, we conducted the partitioning exercise in Fig. 10 mainly to highlight the fact that information on the proportional contribution of above- versus belowground respiration is present in estimates of $\delta^{18}O_R$; there is still a great deal of progress being made on methods of extracting this information. It does appear that the

assumption of 50% contributions of leaf and soil respiration to total ecosystem respiration made in Pataki et al. (2003a) may be invalid for the Eastern foothills site, particularly in the wintertime, but reasonable for the Downtown site (Fig. 10). The spatial and temporal pattern of these results is not unexpected: the Salt Lake City urban forest surrounding the Eastern foothills site is dominated by deciduous species, such that small contributions of leaf respiration are likely in the wintertime. In contrast, downtown Salt Lake City has little exposed soil surface (hence soil sampling was not conducted there) and was therefore hypothesized to be dominated by leaf respiration.

Conclusion

In this study we used spatial and temporal variability in atmospheric CO_2 concentrations, CO_2 isotopes, and water isotopes to infer both patterns of human activities as well as plant and soil processes in urban areas. The relative impacts of natural gas combustion and gasoline combustion were apparent in the C isotope composition of elevated urban CO_2 when combined with O isotopes to quantify the role of biogenic respiration. In addition, the magnitude of the O isotope composition of respiration provided information about evaporative enrichment of water pools, irrigation, and the contribution of leaf versus soil respiration to the atmosphere. By conducting these measurements along an urban to rural gradient, the effects of urbanization and land use on the local C cycle and the isotopic composition of C and water pools could be quantified. Further studies in other urbanized areas are needed to generalize these patterns and to scale the impacts of urbanization to larger regions. Expanding long-term monitoring of CO_2 concentrations and isotopic composition to a variety of land cover types, including urban land cover, can greatly expand our understanding of the C cycle.

Appendix

An example of the Bayesian inversion input data, constraints, and results is given for the dataset collected on January 21, 2004 at the Residential site. C_T, $\delta^{13}C_T$, and $\delta^{18}O_T$ were measured directly and are shown below with the standard deviation in parentheses. C_B, $\delta^{13}C_B$, and $\delta^{18}O_B$ were interpolated from NOAA CMDL data as described in the text. The prior constraints are specified below. For $\delta^{18}O_R$ the constraints were modeled from climatic data and source water measurements as the most depleted expected value for soil respiration and the most enriched expected value for leaf respiration during the sampling period. The unknown values C_N, C_G, C_R, and $\delta^{18}O_R$ were then estimated by sampling the results from equation (5) with a Metropolis-Hastings algorithm as described in the text. The resulting marginal distributions for about 5000 accepted estimates are shown in Figure 11 and the means and standard deviations are given below.

Input data	
C_T	429.1 (3.2)
$\delta^{13}C_T$	–11.1 (0.1)
$\delta^{18}O_T$	38.3 (0.1)
Prior constants	
C_N, C_G, C_R	>0
$C_N + C_G + C_R$	$C_T - C_B$
$\delta^{18}O_R$	$23‰ < \delta^{18}O_R < 30‰$
Final estimates	
C_N	30.0 (4.8)
C_G	10.3 (4.9)
C_R	3.5 (3.1)
$\delta^{18}O_R$	28.5 (0.6)

References

Barbour MM, Cernusak LA, Whitehead D, Griffin KL, Turnbull MH, Tissue DT, Farquhar GD (2005) Nocturnal stomatal conductance and implications for modelling $\delta^{18}O$ of leaf-respired CO_2 in temperate tree species. Funct Plant Biol 32:1107–1121

Bowling DR, McDowell NG, Bond BJ, Law BE, Ehleringer JR (2002) ^{13}C content of ecosystem respiration is linked to precipitation and vapor pressure deficit. Oecologia 131:113–124

Bowling DR, McDowell NG, Welker JM, Bond BJ, Law BE, Ehleringer JR (2003) Oxygen isotope content of CO_2 in nocturnal ecosystem respiration 2. Short-term dynamics of foliar and soil component fluxes in an old-growth ponderosa pine forest. Global Biogeochem Cycles 17. doi: 10.1029/2003GB002082

Bush SE, Pataki DE, Ehleringer JR (2007) Sources of variation in $\delta^{13}C$ of fossil fuel emissions in an urban region. Appl Geochem (in press)

Cernusak LA, Pate JS, Farquhar GD (2002) Diurnal variation in the stable isotope composition of water and dry matter in fruiting *Lupinus angustifolius* under field conditions. Plant Cell Environ 25:898–907

Cernusak LA, Farquhar GD, Wong CS, Stuart-Williams H (2004) Measurement and interpretation of the oxygen isotope composition of carbon dioxide respired by leaves in the dark. Plant Phyiol 136:3350–3363

Cernusak LA, Farquhar GD, Pate JS (2005) Environmental and physiological controls over oxygen and carbon isotope composition of Tasmanian blue gum, *Eucalyptus globulus*. Tree Physiol 25:129–146

Clark-Thorne ST, Yapp CJ (2003) Stable carbon isotope constraints on mixing and mass balance of CO_2 in an urban atmosphere: Dallas metropolitan area, Texas, USA. Appl Geochem 18:75–95

Craig H, Gordon LI (1965) Deuterium and oxygen 18 variations in the ocean and marine atmosphere. In: Tongiorigi E (ed) Stable isotopes in oceanographic studies and paleotemperatures. Consiglio Nazionale Delle Ricerche Laboratorio di Geologia Nucleare, Pisa, pp 9–130

Day TA, Gober P, Xiong FS, Wentz EA (2002) Temporal patterns in near-surface CO_2 concentrations over contrasting vegetation types in the Phoenix metropolitan area. Agric For Meteorol 110:229–245

Ewers BE, Oren R (2000) Analyses of assumptions and errors in the calculation of stomatal conductance from sap flux measurements. Tree Physiol 20:579–589

Farquhar GD, Cernusak LA (2005) On the isotopic composition of leaf water in the non-steady state. Funct Plant Biol 32:293–303

Farquhar GD, Gan KS (2003) On the progressive enrichment of the oxygen isotopic composition of water along a leaf. Plant Cell Environ 26:1579–1597

Farquhar GD, Lloyd J (1993) Carbon and oxygen isotope effects in the exchange of carbon dioxide between plants and the atmosphere. In: Ehleringer JR, Hall AE, Farquhar GD (eds) Stable isotopes and plant carbon–water relations. Academic Press, New York, pp 47–70

Farquhar GD, Lloyd J, Taylor JA, Flanagan LB, Syvertsen JP, Hubick KT, Wong SC, Ehleringer JR (1993) Vegetation effects on the isotope composition of oxygen in atmospheric CO_2. Nature 363:439–443

Flanagan LB, Comstock JP, Ehleringer JR (1991) Comparison of modeled and observed environmental influences on the stable oxygen and hydrogen isotope composition of leaf water in *Phaseolus vulgaris* L. Plant Physiol 96:588–596

Flanagan LB, Brooks J, Varney GT, Berry SC, Ehleringer JR (1996) Carbon isotope discrimination during photosynthesis and the isotope ratio of respired CO_2 in boreal forest ecosystems. Global Biogeochem Cycles 10:629–640

Flanagan LB, Brooks JR, Varney GT, Ehleringer JR (1997) Discrimination against $C^{18}O^{16}O$ during photosynthesis and the oxygen isotope ratio of respired CO_2 in boreal forest ecosystems. Global Biogeochem Cycles 11:83–98

Florkowski T, Korus A, Miroslaw J, Necki J, Neubert R, Schimdt M, Zimnoch M (1998) Isotopic composition of CO_2 and CH_4 in a heavily polluted urban atmosphere and in a remote mountain area (Southern Poland). In: Isotope techniques in the study of environmental change. IAEA, Vienna, pp 37–48

Gehre M, Geilmann H, Richter J, Werner RA, Brand WA (2004) Continuous flow $^2H/^1H$ and $^{18}O/^{16}O$ analysis of water samples with dual inlet precision. Rapid Commun Mass Spectrom 18:2650–2660

Gelfand AE, Smith AFM (1990) Sampling-based approaches to calculating marginal densities. J Am Stat Assoc 85:398–409

Gelman A, Rubin DB (1992) Inference from iterative simulation using multiple sequences. Stat Sci 7:457–511

Geman S, Geman D (1984) Stochastic relaxation, Gibbs distributions and the Bayesian restoration of images. IEEE Trans Pattern Anal Mach Intell 6:721–741

Gill J (2002) Bayesian methods: a social and behavioral approach. Chapman & Hall, CRC, Boca Raton, Fla.

Gillon J, Yakir D (2001) Influence of carbonic anhydrase activity in terrestrial vegetation on the ^{18}O content of atmospheric CO_2. Science 291:2584–2587

Globalview-CO_2 (2005) Cooperative atmospheric data integration project—carbon dioxide. http://www.cmdl.noaa.gov, NOAA CMDL, Boulder, Colo.

Harwood KG, Gillon JS, Roberts A, Griffiths H (1999) Determinants of isotopic coupling of CO_2 and water vapour within a *Quercus petraea* forest canopy. Oecologia 119:109–119

Hastings WK (1970) Monte Carlo sampling methods using Markov chain and their applications. Biometrika 57:97–109

Idso CD, Idso SB, Balling RC (1998) The urban CO_2 dome of Phoenix, Arizona. Phys Geogr 19:95–108

Idso CD, Idso SB, Balling RC (2001) An intensive 2-week study of an urban CO_2 dome in Phoenix, Arizona, USA. Atmos Environ 35:995–1000

Keeling CD (1958) The concentration and isotopic abundances of atmospheric carbon dioxide in rural areas. Geochim Cosmochim Acta 13:322–334

Keeling CD (1961) The concentration and isotopic abundance of carbon dioxide in rural and marine air. Geochim Cosmochim Acta 24:277–298

Koerner B, Klopatek J (2002) Anthropogenic and natural CO_2 emission sources in an arid urban environment. Environ Pollut 116:S45–S51

Lai C, Ehleringer JR, Bond BJ, Paw UKT (2006a) Contributions of evaporation, isotopic non-steady state transpiration and atmospheric mixing on the $\delta^{18}O$ of water vapour in Pacific Northwest coniferous forests. Plant Cell Environ 29:77–94

Lai C, Riley WJ, Owensby CE, Ham JM, Schauer AJ, Ehleringer JR (2006b) Seasonal and interannual variations of carbon and oxygen isotopes of respired CO_2 in a tallgrass prairie: measurements and modeling results from 3 years with contrasting water availability. J Geophys Res 111. doi:10.1029/2005JD006436

Leonard T, Hsu JSJ (1999) Bayesian methods—an analysis for statistics and interdisciplinary researchers. Cambridge University Press, Cambridge

Majoube M (1971) Fractionnement en oxygene 18 et en deuterium entre l'eau et sa vapeur. J Chim Phys 58:1423–1436

Miller JB, Yakir D, White JWC, Tans PP (1999) Measurement of $^{18}O/^{16}O$ in the soil–atmosphere CO_2 flux. Global Biogeochem Cycles 13:761–774

Mortazavi B, Chanton JP (2002) Carbon isotopic discrimination and control of nighttime canopy $\delta^{18}O$-CO_2 in a pine forest in the southeastern United States. Global Biogeochem Cycles 16. doi:10.1029/2000GB001390

Pataki DE, Bowling DR, Ehleringer JR (2003a) The seasonal cycle of carbon dioxide and its isotopic composition in an urban atmosphere: anthropogenic and biogenic effects. J Geophys Res 108:4735

Pataki DE, Ehleringer JR, Flanagan LB, Yakir D, Bowling D, Still CJ, Buchmann N, Kaplan JO, Berry JA (2003b) The application and interpretation of Keeling plots in terrestrial carbon cycle research. Global Biogeochem Cycles 17(1):1022

Pataki DE, Bush SE, Ehleringer JR (2005a) Stable isotopes as a tool in urban ecology. In: Flanagan LB, Ehleringer JR, Pataki DE (eds) Stable isotopes and biosphere–atmosphere

interactions: processes and biological controls. Elsevier, San Diego, Calif., pp 199–216

Pataki DE, Tyler BJ, Peterson RE, Nair AP, Steenburgh WJ, Pardyjak ER (2005b) Can carbon dioxide be used as a tracer of urban atmospheric transport? J Geophys Res 110. doi: 10.1029/2004JD005723

Pataki DE, Alig RJ, Fung AS, Golubiewski NE, Kennedy CA, McPherson EG, Nowak DJ, Pouyat RV, Romero Lankao P (2006a) Urban ecosystems and the North American carbon cycle. Global Change Biol 12:1–11

Pataki DE, Bowling DR, Ehleringer JR, Zobitz JM (2006b) High resolution monitoring of urban carbon dioxide sources. Geophys Res Lett 33:L03813. doi: 03810.01029/02005GL024822

Riley WM, Still CJ, Helliker BR, Ribas-Carbo M, Berry JA (2003) ^{18}O composition of CO_2 and H_2O ecosystem pools and fluxes in a tallgrass prairie: simulations and comparisons to measurements. Global Change Biol 9:1567–1581

Schauer AJ, Lai C, Bowling DR, Ehleringer JR (2003) An automated sampler for collection of atmospheric trace gas samples for stable isotope analyses. Agric For Meteorol 118:113–124

Schauer AJ, Lott MJ, Cook CS, Ehleringer JR (2005) An automated system for stable isotope and concentration analyses of CO_2 from small atmospheric samples. Rapid Commun Mass Spectrom 19:359–362

Sternberg LL, Moreira MZ, Martinelli LA, Victoria RL, Barbosa EM, Bonates LCM, Neptad D (1998) The relationship between $^{18}O/^{16}O$ and $^{13}C/^{12}C$ ratios of ambient CO_2 in two Amazonian tropical forests. Tellus 50B:366–376

Tarantola A (2005) Inverse problem theory and model parameter estimation. SIAM, Philadelphia, Pa.

West AG, Patrickson SJ, Ehleringer JR (2006) Water extraction times for plant and soil materials used in stable isotope analysis. Rapid Commun Mass Spectrom 20:1317–1321

Xu T, White D, Hui D, Luo Y (2006) Probabilistic inversion of a terrestrial ecosystem model: analysis of uncertainty in parameter estimation and model prediction. Global Biogeochem Cycles 20. doi: 10.1029/2005GB002468